

# Geophysical Research Letters<sup>®</sup>



## RESEARCH LETTER

10.1029/2021GL094143

### Key Points:

- Devolatilization of early Europa's rocky interior may have generated a mildly acidic ocean
- Heating drove outgassing of up to 1–270 bar CO<sub>2</sub>, perhaps as an early atmosphere since lost, or captured as a large clathrate reservoir
- Calcium, sulfate, and carbonate salts precipitate at the seafloor, while chloride is abundant nearer the ice shell

### Supporting Information:

Supporting Information may be found in the online version of this article.

### Correspondence to:

M. Melwani Daswani,  
[mohit.melwani.daswani@jpl.caltech.edu](mailto:mohit.melwani.daswani@jpl.caltech.edu)

### Citation:

Melwani Daswani, M., Vance, S. D., Mayne, M. J., & Glein, C. R. (2021). A metamorphic origin for Europa's ocean. *Geophysical Research Letters*, 48, e2021GL094143. <https://doi.org/10.1029/2021GL094143>

Received 7 MAY 2021

Accepted 4 AUG 2021

© 2021 Jet Propulsion Laboratory, California Institute of Technology. Government sponsorship acknowledged.

This is an open access article under the terms of the [Creative Commons Attribution-NonCommercial License](https://creativecommons.org/licenses/by-nc/4.0/), which permits use, distribution and reproduction in any medium, provided the original work is properly cited and is not used for commercial purposes.

## A Metamorphic Origin for Europa's Ocean

Mohit Melwani Daswani<sup>1</sup> , Steven D. Vance<sup>1</sup> , Matthew J. Mayne<sup>2</sup> , and Christopher R. Glein<sup>3</sup> 

<sup>1</sup>Jet Propulsion Laboratory, California Institute of Technology, Pasadena, CA, USA, <sup>2</sup>Department of Earth Sciences, Stellenbosch University, Stellenbosch, South Africa, <sup>3</sup>Space Science and Engineering Division, Southwest Research Institute, San Antonio, TX, USA

**Abstract** Europa likely contains an iron-rich metal core. For it to have formed, temperatures within Europa reached  $\gtrsim 1250$  K. Going up to that temperature, accreted chondritic minerals — for example, carbonates and phyllosilicates — would partially devolatilize. Here, we compute the amounts and compositions of exsolved volatiles. We find that volatiles released from the interior would have carried solutes, redox-sensitive species, and could have generated a carbonic ocean in excess of Europa's present-day hydrosphere, and potentially an early CO<sub>2</sub> atmosphere. No late delivery of cometary water was necessary. Contrasting with prior work, CO<sub>2</sub> could be the most abundant solute in the ocean, followed by Ca<sup>2+</sup>, SO<sub>4</sub><sup>2-</sup>, and HCO<sub>3</sub><sup>-</sup>. However, gypsum precipitation going from the seafloor to the ice shell decreases the dissolved S/Cl ratio, such that Cl>S at the shallowest depths, consistent with recently inferred endogenous chlorides at Europa's surface. Gypsum would form a 3–10 km thick sedimentary layer at the seafloor.

**Plain Language Summary** It is likely that Jupiter's moon Europa hosts a deep ocean underneath its surface ice shell. Telescopes and spacecraft have observed chlorine-bearing salts on the surface, but we do not yet know what they mean for the chemical composition of the ocean, or how the ocean came to be. Here, we test whether the breakdown of minerals containing volatile elements (hydrogen, carbon, sulfur, and chlorine) inside Europa might have released enough water to produce the ocean. The breakdown of these minerals generally happens at high temperature, but how hot did Europa's interior get? NASA's Galileo spacecraft confirmed that Europa probably has an iron-rich core, and such cores can only form at high temperature: at least 1250 K. Knowing this, we model the effect that heat had on the minerals (a process known as metamorphism) and calculate how much water would be released, as volatile-rich minerals transform into volatile-free minerals. We find that this process could release massive amounts of carbon dioxide, more than enough water to form Europa's present ocean, and produce sulfate and carbonate minerals. Chlorine released would be more abundant in the ocean's shallower depths, perhaps explaining the telescope observations.

## 1. Introduction

Key to understanding the past and present habitability of Jupiter's moon Europa is its composition and evolution. Europa hosts a  $\gtrsim 100$  km deep liquid water ocean beneath its 3–30 km ice shell (e.g., Schubert et al., 2009). Water, solutes and possible oxidants needed to carry out metabolic processes (Gaidos et al., 1999; Hand et al., 2007) in Europa's ocean were delivered through some combination of Europa's accreted materials, release by subsurface geochemical reactions, and subsequently by meteoritic or Io-genic influx.

Surface spectra were initially interpreted as hydrated surface salts from a sulfate-rich ocean (McCord et al., 1998), consistent with models of brine evolution in CI chondrite bodies (Kargel, 1991; Kargel et al., 2000; Zolotov & Shock, 2001). These models propose that Europa's ocean evolved from a reduced Na-Cl-dominated composition to a more oxidized Mg-sulfate ocean as a result of: (a) thermodynamic equilibrium (including by hydrothermal activity) between the ocean and silicate interior, while reduced volatiles H<sub>2</sub> and CH<sub>4</sub> produced by water-rock interaction escaped (Zolotov & Kargel, 2009; Zolotov & Shock, 2001, 2004); and/or (b) large fluxes of surface-derived oxidants delivered into the ocean through overturning of the icy lithosphere (Hand et al., 2007; Pasek & Greenberg, 2012). Recently, however, a sulfate-rich ocean has been challenged because the interpretation of hydrated sulfate salts on the surface as an oceanic signature is not apparently consistent with more recent spectroscopic observations. These observations favor instead

chloride salts on the most geologically disrupted surfaces; surface sulfate salts and hydrated sulfuric acid are interpreted as radiolytic end-products (Brown & Hand, 2013; Fischer et al., 2016; Ligier et al., 2016; Trumbo et al., 2019, 2017, but cf., Dalton et al., 2013). Alternatively, the ocean may have remained reduced and sulfidic if H<sub>2</sub> and CH<sub>4</sub> escape to space was limited (McKinnon & Zolensky, 2003).

Here, we use geochemical and petrologic models to assess whether planetary-scale thermal processes were responsible for the build-up of Europa's ocean, and whether thermal evolution of the deep interior had a significant impact on the composition of the ocean. While plausible models of Europa have been constructed without a solid iron-rich core (Table S1), Europa's high density and the inferred molten iron core in neighboring Ganymede (Bland et al., 2008) strongly suggest a high-temperature history for Europa's interior (e.g., Greeley et al., 2004; Tobie et al., 2003, 2005) consistent with the formation of an iron-rich core (Anderson et al., 1998; Moore & Hussmann, 2009; Schubert et al., 2009). The decay of short-lived radionuclides in the accreting material could have heated the silicate interior sufficiently for partial melting to separate silicate and metal (cf., Barr & Canup, 2008), or to at least expel volatiles, as occurred during the thermal metamorphism of some chondrites (e.g., Huss et al., 2006). Additionally, tidal dissipation during Europa's orbital evolution may have affected early heating and differentiation of the interior at a level comparable to radiogenic heating, but disentangling the influence of tidal dissipation from other early sources of heat is difficult (Hussmann & Spohn, 2004).

If Europa has a Fe-rich core, then a fraction of the deep interior was heated at least to the Fe ± S eutectic temperature during differentiation. Accordingly, we hypothesize that prograde metamorphism (i.e., metamorphic changes caused by increasing temperature) and associated chemical reactions in the deep interior were the driving forces behind the ocean's formation and its composition. Based on this prograde assumption for Europa's evolution we: (a) establish a starting bulk composition of Europa immediately after accretion using an accretion model and compositional endmember scenarios; (b) use a Gibbs free energy minimization petrologic model to constrain a range of compositions for the changing ocean and deep interior during thermal excursions that could be caused by differentiation and/or thermal-orbital evolution (e.g., Hussmann & Spohn, 2004; Tobie et al., 2005); (c) use a chemical equilibrium model to calculate the composition of Europa's ocean after its generation by metamorphic reactions; and (d) constrain the present composition and interior structure of Europa by using mass balance and a 1D interior structure model consistent with Europa's gravitational coefficients and moment of inertia (MoI).

## 2. Methods

A flow chart summarizing the methods below is shown in Figure S1.

### 2.1. Bulk Composition of the Accreted Body

To date, accretion models have suggested that Europa's bulk water content was derived from dust, pebbles or satellitesimals composed of non-hydrated silicate, plus varying amounts of water ice as a function of the (possibly migrating) position of the circumjovian snow line toward the late stages of accretion (e.g., Canup & Ward, 2002, 2009; Lunine & Stevenson, 1982; Makalkin et al., 1999; Ronnet et al., 2017), and/or capture and impact processing (e.g., Estrada et al., 2009; Mosqueira et al., 2010; Ronnet & Johansen, 2020). Both scenarios can lead to bodies consistent with models of the density gradient in the Galilean satellites and orbital properties, but rely on the fortuitous delivery of the exact mass of water as ice to explain the present-day hydrosphere (8–12 wt.%) despite widely different sizes ( $\sim 10^{-3}$ – $10^5$  m radius) and water ice contents (0.571–50 wt.%; Ronnet & Johansen, 2020; Ronnet et al., 2017) of the accreting particles. A recent reappraisal of hydrodynamic escape during accretion also yields water contents and densities consistent with present day observations (Bierson & Nimmo, 2020). The alternative that we explore here is one where variable amounts of water and volatiles are already present in Europa's accreting particles, based on the compositions of the proposed silicate-rich building blocks of Europa (i.e., chondrites) according to geophysical and geochemical models (Kargel et al., 2000; Kuskov & Kronrod, 2005; McKinnon & Zolensky, 2003; Zolotov & Kargel, 2009; Zolotov & Shock, 2001), and tie the subsequent thermal evolution of the accreted body to present-day Europa's spherical structure and gravitational MoI. Chondrites contain various amounts of volatiles in minerals and organics (Table S2), the thermal processing of which could yield sufficient mass to form

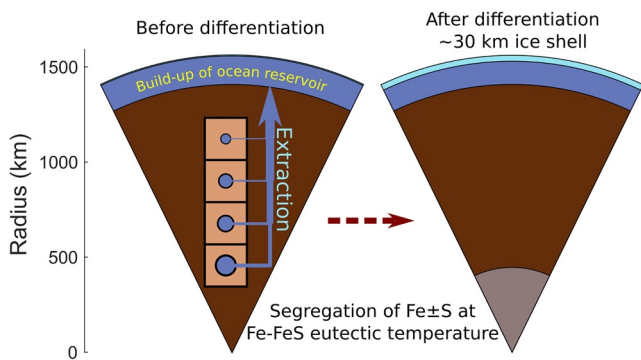


**Figure 1.** Schematic of the thermodynamic + extraction + structure model to simulate the build-up of Europa's ocean from exsolved volatiles. After each heating step before differentiation, Gibbs energy minimization is carried out, resulting in an equilibrium assemblage in each cell (left figure). A portion of the fluid phase(s) is then extracted according to a specified rule (see Section 2.2), joins the ocean reservoir, and no longer affects the chemistry of the deep interior. Fe ± S is extracted from the bulk composition from the deep interior once the interior reaches the Fe-FeS eutectic temperature (Section 2.3). Finally, Europa's structure is resolved (Section 2.4), here assuming a 30 km ice shell, requiring a temperature of 270.8 K at the ice-ocean interface.

the present-day hydrosphere and still fulfill the geophysical constraints. A present-day hydrated silicate interior for Europa is implausible given gravity and density measurements (Anderson et al., 1998; Kuskov & Kronrod, 2005; Schubert et al., 2009; Sohl et al., 2002; Vance et al., 2018), so subsequent thermal processing, nominally differentiation of the body will be necessary to meet the constraints.

The composition and water mass fraction for the initial state of Europa before differentiation (*MC-Scale*) are estimated using a Monte Carlo accretion model (AccretR). Additionally, we consider two endmember compositions: one in which Europa accreted entirely from CI carbonaceous chondrites (*EM-CI*), and another in which Europa accreted from CM chondrites only (*EM-CM*).

The models are insensitive to the mineralogy of the initial pebbles/satellitesimals and whether these were in thermochemical equilibrium prior to accretion (McKinnon & Zolensky, 2003) because our calculations of the subsequent geochemical evolution of these materials depend on the bulk composition, not the mineralogy. Nevertheless, hydrous minerals in planetesimal collisions are predicted to survive without substantial dehydration (Wakita & Genda, 2019). Further details about the accretion and composition models, and an additional model exploring a hypothetical reduced CI chondrite body are shown in Text S1 and Figures S4 and S5, and the initial bulk compositions are summarized in Table S3.

## 2.2. Ocean Build-Up by Prograde Metamorphism Until the Onset of Core Formation

To determine the mass and composition of an ocean produced during heating, devolatilization, and differentiation of the deep interior, we use the *Perple\_X* Gibbs free energy minimization program, which leverages experimental and modeled thermodynamic data, including non-aqueous solvents, and the *Deep Earth Water* model optimized for computing aqueous fluid speciation at high pressure (e.g., Connolly, 2005, 2009; Connolly & Galvez, 2018; Galvez et al., 2015; Pan et al., 2013). For each initial bulk composition (Section 2.1), we model a 0-dimensional heating pathway throughout the deep interior using *Rcrust* (Mayne et al., 2016), which provides an interface to model complex phase fractionation. We construct a 1D column spanning the radius of Europa discretized into a number of vertical cells that experience isobaric heating steps, and track the composition and mass of the equilibrium mineral-plus-volatile assemblage. At each heating step ( $\Delta T$ ), the Gibbs energy of the assemblage in each cell is minimized, resulting in a new equilibrium assemblage that depends on the heating step directly prior to it, but is not affected by the adjacent vertical cells.

We simulate the build-up of the ocean by imposing a limit on the fraction of volatiles retained in the assemblage for each heating step. That is, if fluids (except silicate melt, see below) are thermodynamically stable, a specified portion is irreversibly fractionated from the equilibrium assemblage of the particular cell to go into the growing ocean reservoir (Figure 1). As a limiting case, for each bulk composition computed (Section 2.1) we apply our thermodynamic models with a retained-to-extracted (R/E) fluid mass ratio of 0, that is, all fluids (including gases, liquids and their dissolved species) produced during heating are extracted from the interior. Buoyancy drives fluids upward, with transport being particularly rapid in permeable materials in the direction of maximum compressive stress (e.g., Richard et al., 2007). Long-term retention of fluids at high pressure would lead to an unstable solution that is out of hydrostatic equilibrium. Thus, the only path for free low density fluids is up. This efficient extraction of volatiles from Europa's interior is consistent with findings for the more limiting case of Titan (Leitner & Lunine, 2019) where a volatile-rich hydrosphere and atmosphere were formed endogenously (Miller et al., 2019; Néri et al., 2020) despite higher overburden pressure and gravity, and reduced tidal heating, that would more efficiently prevent their escape.

The CI chondrite endmember bulk composition modeled for Europa would contain water in excess of Europa's present hydrosphere (Section 2.1), so for *EM-CI*, we also test the effect of varying the R/E fluid mass ratio, and carry out a model with a R/E ratio of 0.1 at each heating step, that is, at each  $\Delta T$ , thermodynamic equilibrium is computed, and subsequently 1 part of fluid is retained for 10 parts of fluid extracted. For *EM-CI* we also test the effect of a constant mass of fluid present in the rocky interior by retaining 5 wt.% fluid and extracting any fluid in excess, similar to how magma chambers reach a critical size threshold prior to eruption (e.g., Townsend & Huber, 2020) (See Text S2 for model parameters and validation, and Table S4 for activity-composition models used.) As discussed, Europa likely contains a Fe-rich core, so the lowest maximum temperature the interior reached during prograde metamorphism is the melting temperature of the Fe-rich phase(s) that eventually formed the core (Section 2.3). Therefore, the resulting concentrations we report here represent a lower limit of the exsolved and extracted volatiles that formed Europa's proto-ocean. The onset of differentiation occurs at a temperature lower than the temperature of silicate melting (Section 2.3), hence silicate partial melting does not occur here.

### 2.3. Core Composition

In our model we assume that prograde metamorphism proceeded at least up to the Fe-FeS eutectic temperature in order for core formation to proceed. Since this occurs at temperatures higher than volatile-releasing metamorphic reactions (see Section 2.2), we further assume that core formation does not appreciably sequester volatiles that would build the ocean. Our calculations are performed in the simplified Fe-S system as an initial approximation for an expected core composition, mass and density, until a future mission can constrain the deep interior composition of Europa from its seismic properties and improved gravity data. For further details on assumptions taken for modeled temperatures and the chemical system considered see Text S3.

### 2.4. Post-Differentiation Structure, Mineralogy and Geochemistry

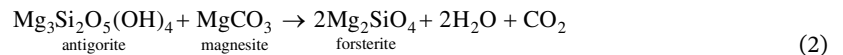
We obtain our final predictions for Europa's interior structure after the formation of the ocean and differentiation using PlanetProfile, a program for constructing 1D planetary structure models, in which the self-consistent gridded thermodynamic properties from *Perple\_X* and *Rcrust* are used as inputs (Vance et al., 2018). To construct the inputs, we first use *Rcrust* to perform isobaric heating simulations as described in Section 2.2 and Figure 1 to obtain the thermodynamic properties. We then remove the appropriate Fe  $\pm$  S mass from the silicate layer for each model Europa to form a core with 24 mass % sulfur (the minimum amount of sulfur in melt at the Fe-FeS eutectic within Europa, see Section 2.3) for *EM-CI*, *EM-CM* and *MC-Scale* after fluid extraction up to the Fe-FeS eutectic temperature (Section 2.2). Finally, we fold the separate silicate layer and Fe  $\pm$  S core (Section 2.3) thermodynamic properties into PlanetProfile and obtain structures consistent with Europa's radius, density and MoI. Text S4 describes inputs and modifications to PlanetProfile for this work. The results form a baseline against which spacecraft observations may be compared to elucidate the effects of  $\sim 4.5$  Gyr of orbital-geologic history.

### 2.5. Ocean Column Composition

We use the bulk extracted ocean compositions and masses (Section 2.2) as inputs into geochemical model CHIM-XPT (Reed, 1998) to compute ocean depth dependent mineral-aqueous solution-gas equilibria using the self-consistent thermodynamic database SOLTHERM, which includes thermodynamic properties of water and equilibrium constants up to 0.5 GPa. We carry out a 1D CHIM-XPT model for the bulk fluids extracted by prograde metamorphism of *EM-CI*, *EM-CM*, and *MC-Scale* (Section 2.2), varying the pressure from the seafloor (200 MPa; Vance et al., 2018) up to a hypothetical ice-free surface. This way, we quantify gas saturation and mineral precipitation out of the primordial ocean (i.e., fractionation), and the effects on the water column's composition, pH and redox potential. Further details about CHIM-XPT and validation of the model are found in Text S2.

### 3. Results and Discussion

Prograde metamorphism up to the Fe-FeS eutectic temperature has the effect of dehydrating, dehydroxylating, decarbonizing and desulfurizing the deep interior, irreversibly changing the mineralogy (e.g., Glein et al., 2018). The main volatile-releasing generalized reactions are:



Large amounts of volatiles are released at low temperature (< 300 K): the starting rock compositions (namely volatile-rich carbonaceous chondrites) are thermally unequilibrated, so the thermodynamic model predicts that excess volatiles (mainly water and CH<sub>4</sub>) and dissolved solutes are unbound from minerals and organics. At moderate temperatures (300–600 K), only small amounts of fluid are released because lizardite, antigorite, chlorite and magnesite are stable; these are phyllosilicate or carbonate minerals with structurally bound water and OH<sup>-</sup>, or CO<sub>3</sub><sup>2-</sup>. At ≳ 650 K, antigorite and magnesite break down, releasing H<sub>2</sub>O and CO<sub>2</sub>. Higher pressure stabilizes magnesite and antigorite, whereas lower pressure favors their breakdown at that temperature. Analogous volatile-releasing reactions occur presently in Earth's subducting oceanic plates, for example, which experience dewatering and decarbonization with increasing pressure and temperature (e.g., Gorce et al., 2019; Manthilake et al., 2016). Further details about the pressures and temperatures of the reactions and the changing mineralogy along the prograde metamorphic path are found in Text S5 and Figures S12 and S13.

#### 3.1. Extracted Fluid Compositions and Ocean Masses

Prograde metamorphism of the *EM-CI* and *EM-CM* initial compositions supplies a fluid mass that exceeds the present ~ 10 wt. % hydrosphere for all tested R/E ratios. The *MC-Scale* composition however, is unable to supply sufficient fluid mass, despite a R/E ratio = 0, since the maximal water content of this composition (3.5 ± 0.6 wt.%, assuming all H is in H<sub>2</sub>O) falls short of Europa's present hydrosphere mass, indicating that additional water was co-accreted or delivered if Europa formed from the materials nearest to Jupiter ~ 4.5 Ga according to the MC accretion model (Section 2.1).

The pattern of volatile release at different pressures and temperatures is broadly similar for all prograde metamorphism models of the initial compositions tested. We focus on solutes and solvents from *EM-CM* shown in Figure 2, and include additional subtleties of the exsolved fluid compositions in Text S5, Table S5 and Figures S6–S11. In all cases, the most significant contributors to the ocean reservoir mass are oxygen and hydrogen, as water (e.g., Figure 2). Carbon is the third most abundant element comprising the ocean reservoir of the *EM-CI* and *EM-CM* models, particularly at relatively high temperatures where CO<sub>2</sub> becomes a major component, and acts as the solvent, in the fluid phase (Figure 2) as a result of carbonate destabilization (see also Section 3.3). However, while carbon, hydrogen, oxygen, sulfur, and calcium abundances in the exsolved ocean reservoirs of *EM-CI* and *EM-CM* are comparable, the total mass of silicon, sodium, magnesium, chlorine, potassium and aluminum extracted from *EM-CM* is significantly higher, and only the extracted mass of iron is lower after prograde metamorphism of *EM-CM* compared to *EM-CI*. For *MC-Scale*, the most abundant solutes in the extracted ocean are calcium and sulfur, especially exsolved at <650 K and >6 GPa in the form of CaSO<sub>4</sub>, although some calcium is paired to chlorine, as CaCl<sub>2</sub>.

#### 3.2. Composition of the Ocean Column, Precipitated Minerals and Exsolved Gases

Distinct ocean compositions from seafloor to surface (Figure 3) result from isothermal 1D decompression CHIM-XPT models equilibrating the bulk compositions of the extracted fluids for *EM-CI*, *EM-CM*, and *MC-Scale* (Section 3.1). In all cases, gypsum (CaSO<sub>4</sub>) saturates and precipitates as pressure decreases. Additionally, for *EM-CM*, dolomite is stable throughout the water column, while for *MC-Scale*, dolomite is stable at < 30 MPa, which may correspond to a depth within the present ice shell (Figure 3). Since prograde metamorphism of the *MC-Scale* composition did not yield a sufficiently massive hydrosphere (Section 3.1), we consider the effects of compensating the difference with late delivery of cometary materials in Text S7 and Figure S15.

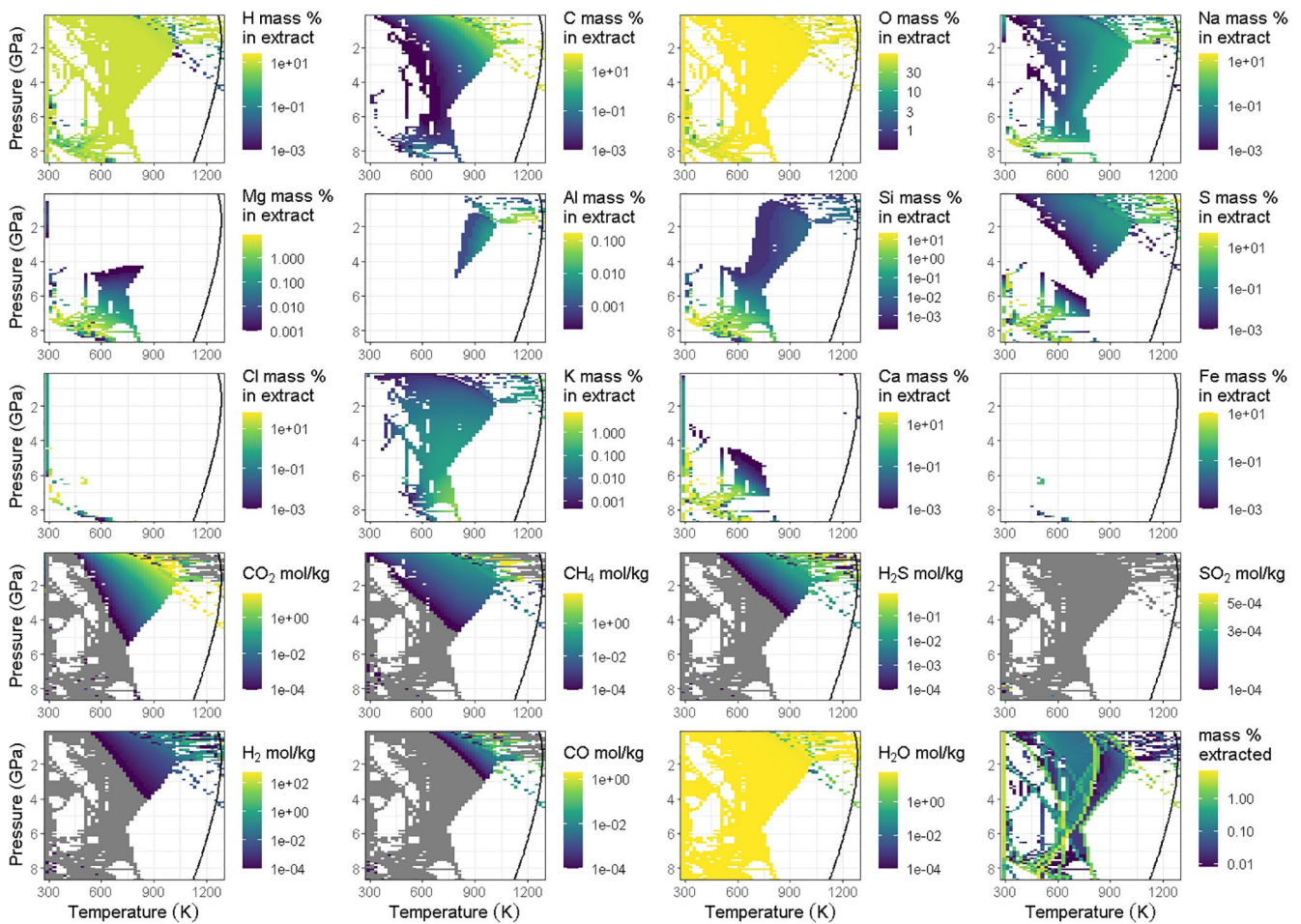


**Figure 2.** Composition of the fluid extracted from the deep interior at different pressures with increasing temperature for the endmember model "Europa accreted from CM chondrites" (*EM-CM*), retained-to-extracted ratio ( $R/E$ ) = 0. Solid curves show the Fe-FeS eutectic temperature. Integrating up to the eutectic yields the total amounts exsolved from the deep interior. Blank areas signify that no fluids containing the specific element shown in the plot were extracted at those pressures and temperatures. Rows 1–3: elemental abundance of the extracted fluid (solvents and solutes). Rows 4 and 5: molecular solvent moles per kilogram of extracted fluid. Gray areas in the solvent plots signify that fluids were extracted at those pressures and temperatures, but did not contain the specific compound shown in the plot. Bottom-right plot: total (solvent + solute) extracted mass. For corresponding figures of the broadly similar patterns of exsolution in the endmember "Europa accreted from CI chondrites" (*EM-CI*) and Monte Carlo (*MC*)-Scale models, see Figures S7–S10.

Gypsum precipitation throughout the water column steadily decreases the S/Cl molar ratio with decreasing depth in all cases, such that the total concentrations of chlorine and sulfur become comparable ( $\Sigma Cl \approx \Sigma S$ ) at shallow depths for *EM-CI* and *EM-CM* (Figure 3), and chlorine exceeds sulfur at  $\lesssim 124$  MPa for *EM-CI*. Similarly, the dissolved calcium concentration decreases as a result of gypsum precipitation, decreasing the Ca/Mg molar ratio with decreasing depth in all models. No Na- or K-bearing minerals saturate, so the Na/K molar ratio remains constant at all depths. In the limiting assumption of zero porosity, the globally averaged thickness of all mineral precipitates at Europa's seafloor is 2.7–9.5 km (Table 1).

The combined mass of gases (particularly  $CO_2$ ) that would boil out of the ocean at low pressure (i.e., at  $< 20$  MPa for a hypothetical non-ice covered surface) is comparable to the mass of precipitated minerals (Figure 3 and Table 1). The massive outgassing of volatiles (0.06%–1.33% Europa's mass; Table 1) may have led to an early  $CO_2$ -rich atmosphere of considerable thickness, on the order of 1–27 MPa for the mass of exsolved gases calculated if they were released all at once. We note that 5–25 MPa of  $H_2O$  and in excess of 1–5.5 MPa of  $CO_2$  are calculated to have been lost from Mars  $< 12$  Myr after accretion (Erkaev et al., 2014; Odert et al., 2018). Massive primordial atmospheres have also been predicted for Triton ( $\sim 16$  MPa  $pCO_2$ ; Lunine & Nolan, 1992), Titan, Ganymede and Callisto (Kuramoto & Matsui, 1994). With such a thick atmosphere, greenhouse trapping of heat generated by insolation (Zahnle & Catling, 2017), radioactive decay

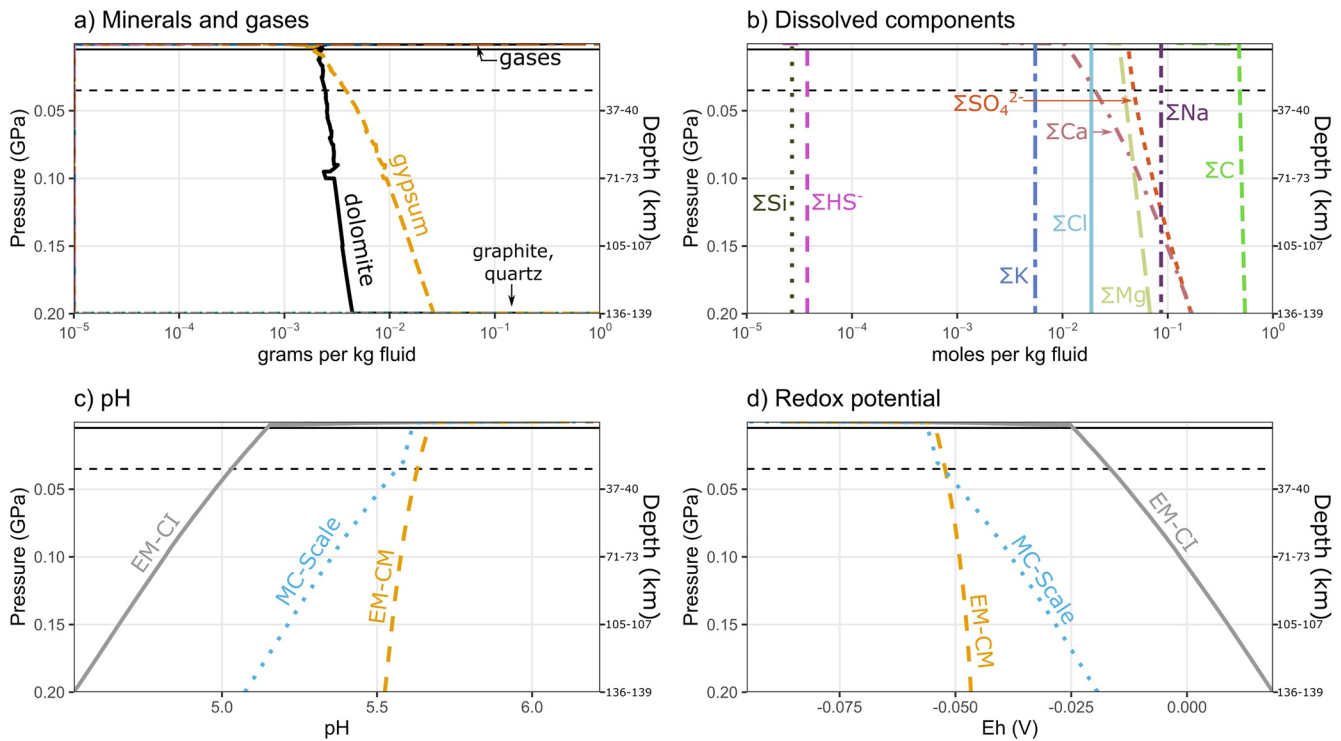


**Figure 3.** Ocean column compositions from the seafloor to the surface, for endmember Europa accreted from CM chondrites (*EM-CM*). Solid and dashed horizontal lines show the pressure at the base of a current 5 and 30 km ice shell respectively (see Section 3.3). (a) Minerals precipitated and gases exsolved with decreasing depth in the water column. (b) Total dissolved components in the water column. Dissolved components shown here are the sum of those particular components distributed among all species in solution. For example, component  $\Sigma C$  represents the sum of carbon in aqueous  $HCO_3^-$ ,  $CH_4$ ,  $CO_2$ , and organics, among other species. Concentrations  $< 10^{-5}$  mol/kg not shown. (c) pH, and (d) redox potential of the ocean column for the retained-to-extracted ratio ( $R/E = 0$ ) models of Europa accreted from CI carbonaceous chondrites (*EM-CI*), *EM-CM*, and Monte Carlo (*MC*)-Scale.

or tides would likely vaporize Europa's hydrosphere, although exceedingly high rates of atmospheric escape by thermal and non-thermal processes, including ionization in Jupiter's magnetosphere, sputtering by solar energetic particles and galactic cosmic rays, or impact erosion, would have likely either prevented atmospheric build-up, or allowed recondensation of the hydrosphere. We do not quantify the lifetime or stability of a possible early steam atmosphere here, but note that up to 27 MPa of  $H_2O + CO_2$  would have been available from metamorphic reactions and subsequent exsolution from the ocean.

More likely, the rate of heating (radioactive or tidal) would control the rate of exsolution from the deep interior, ocean build-up, and the subsequent mass outgassed from the ocean. Based on mass ejection rates from tentative plume detections (Roth et al., 2014; Sparks et al., 2016), plumes could output up to  $7.2 \times 10^{19}$ – $7.2 \times 10^{20}$  kg of  $H_2O$  over the lifetime of the solar system, or about 1.4%–24% of Europa's present ocean mass (Text S6). Alternatively, clathrate hydrates could trap dissolved carbon and limit  $CO_2$  outgassing. Whether  $CO_2$  clathrates are stable in Europa's ocean depends on the pressure and temperature, assuming sufficient  $CO_2$  feedstock is present. For the large amounts of  $CO_2$  produced here, we predict structure I clathrates with a  $CO_2/H_2O$  molar ratio of 0.159 at 273.15 K and equilibrium pressure (1.24 MPa), with a density of 1106 kg/ $m^3$  (see Text S6 for details). This exceeds the ocean's density, so these clathrates would sink, forming a 3.4–77 km layer on the seafloor. The thermal blanketing effect of a thick clathrate layer may ultimately freeze the ocean, which is inconsistent with the present-day state of the ocean. However, the long term stability of such a clathrate layer may be unfavorable because: (a) temperatures  $> 299$  K preclude  $CO_2$  clathrate stability in Europa's ocean (Text S6 and Figure S14), and magmatic episodes are predicted at Europa's seafloor over geologic time (Běhounková et al., 2021), and (b) formation of the ice shell would further increase the salinity and density of the ocean, inhibiting the formation of clathrates or making them buoyant.

We find major differences between the ocean compositions predicted here and those presented previously. On the basis of thermodynamic equilibrium and extensive water-rock interaction between the ocean and the sea-

**Table 1**

Adjusted Mass of Europa's Hydrosphere After Accounting for Sediments Predicted to Precipitate on the Seafloor and Mass of Gases Exsolved at low Pressure in the Ocean Column

Mineral precipitates	<i>EM-CI</i> R/E = 0		<i>EM-CM</i> R/E = 0		<i>MC-Scale</i> R/E = 0	
	Concentration g/kg fluid	Mass kg	Concentration g/kg fluid	Mass kg	Concentration g/kg fluid	Mass kg
graphite	3.92	$3.82 \times 10^{19}$	3.93	$2.75 \times 10^{19}$	5.34	$6.89 \times 10^{18}$
pyrite	0.02	$2.17 \times 10^{17}$	0	0	0.26	$3.35 \times 10^{17}$
quartz	2.59	$2.52 \times 10^{19}$	8.51	$5.96 \times 10^{19}$	1.20	$1.55 \times 10^{18}$
sulfur	0.78	$7.63 \times 10^{18}$	0	0	0	0
gypsum	50.08	$4.89 \times 10^{20}$	34.46	$2.41 \times 10^{20}$	117.09	$1.51 \times 10^{20}$
dolomite	3.28	$3.20 \times 10^{19}$	7.84	$5.49 \times 10^{19}$	2.86	$3.68 \times 10^{18}$
Total precipitates	Mean density kg/m <sup>3</sup>	Thickness km	Mean density kg/m <sup>3</sup>	Thickness km	Mean density kg/m <sup>3</sup>	Thickness km
	2,305 <sup>a</sup>	9.5 <sup>a</sup>	2,413	6.2	2,300 <sup>a</sup>	2.7 <sup>a</sup>
Gases exsolved	<i>EM-CI</i> R/E = 0		<i>EM-CM</i> R/E = 0		<i>MC-Scale</i> R/E = 0	
	Concentration g/kg fluid	Mass kg	Concentration g/kg fluid	Mass kg	Concentration g/kg fluid	Mass kg
H <sub>2</sub> O gas	$2.90 \times 10^{-2}$	$2.83 \times 10^{17}$	$1.81 \times 10^{-2}$	$1.27 \times 10^{17}$	$2.06 \times 10^{-2}$	$2.66 \times 10^{16}$
CO <sub>2</sub> gas	65.58	$6.40 \times 10^{20}$	14.86	$1.04 \times 10^{20}$	20.53	$2.65 \times 10^{19}$
CH <sub>4</sub> gas	$2.66 \times 10^{-8}$	$2.59 \times 10^{11}$	$5.90 \times 10^{-9}$	$4.13 \times 10^{10}$	$4.32 \times 10^{-8}$	$5.57 \times 10^{10}$
H <sub>2</sub> gas	$6.37 \times 10^{-10}$	$1.34 \times 10^9$	$3.72 \times 10^{-10}$	$2.60 \times 10^9$	$6.50 \times 10^{-10}$	$8.38 \times 10^8$
H <sub>2</sub> S gas	$1.38 \times 10^{-3}$	$1.34 \times 10^{16}$	$5.66 \times 10^{-4}$	$3.96 \times 10^{15}$	$1.89 \times 10^{-3}$	$2.44 \times 10^{15}$
Total gases exsolved	Mass (kg)		Mass (kg)		Mass (kg)	
	$6.40 \times 10^{20}$		$1.04 \times 10^{20}$		$2.65 \times 10^{19}$	
Adjusted hydrosphere (A <sub>Hyd</sub> )	<i>EM-CI</i> R/E = 0		<i>EM-CM</i> R/E = 0		<i>MC-Scale</i> R/E = 0	
	Mass kg	A <sub>Hyd</sub> /M <sub>Eur</sub> Mass%	Mass kg	A <sub>Hyd</sub> /M <sub>Eur</sub> Mass%	Mass kg	A <sub>Hyd</sub> /M <sub>Eur</sub> Mass%
	$8.56 \times 10^{21}$	17.83	$6.51 \times 10^{21}$	13.57	$1.26 \times 10^{21}$	2.63

Note. *EM-CI* = endmember CI initial bulk composition, *EM-CM* = endmember CM initial bulk composition, *MC-Scale* = Monte Carlo scaled initial composition, R/E = fluid retained-to-extracted mass ratio. "Thickness" = globally averaged thickness of the precipitate layer at Europa's seafloor, for a hydrosphere depth of 140 km (see Section 3.3). "Adjusted hydrosphere mass" = mass of exsolved volatiles from the interior (Section 3.1) minus the mass of minerals precipitated and gases exsolved from the water column. M<sub>Eur</sub> = mass of Europa.

<sup>a</sup>Does not include dolomite precipitated, since it is not thermodynamically stable at the seafloor of *EM-CI* (see Section 3.2).

floor, Zolotov and Kargel (2009) predicted a "low pH" fluid that rapidly (~ 10<sup>6</sup> yr) evolved to a reduced and basic primordial ocean (pH = 13–13.6) rich in H<sub>2</sub>, Na<sup>+</sup>, K<sup>+</sup>, Ca<sup>2+</sup>, OH<sup>-</sup>, and Cl<sup>-</sup>. The escape of H<sub>2</sub> may have then led to a progressively oxidized, sulfate-rich ocean today. On the other hand, work by Kargel et al. (2000) and Zolotov and Shock (2001) on the low temperature aqueous differentiation, brine evolution, and freezing of the European ocean broadly coincides with our predictions for a sulfate- and carbonate-rich ocean, although they predict that the most abundant cation in solution would be Mg<sup>2+</sup> instead of Ca<sup>2+</sup>. Hansen and McCord (2008) also favored a CO<sub>2</sub>-rich ocean based on spectroscopic observations. If the acidic ocean predicted here could subsequently react and rehydrate the silicate interior, sulfate reduction to sulfide in the presence of reductants would be a kinetically favored sulfur sequestration reaction (Tan et al., 2021), and potentially CO<sub>2</sub> could be converted to CH<sub>4</sub> or graphite.

We also find it significant that the composition of the ocean column is depth-dependent, such that anion and cation concentrations, pH, and redox conditions close to the seafloor are not apparently reflective of the

composition nearer to the surface or at the base of the ice shell. A caveat is that the results presented here do not account for homogenizing or mixing of the ocean column's composition by advection or convection, or latitudinal changes; a comprehensive ocean circulation model (e.g., Lobo et al., 2021) would be required to place such constraints.

### 3.3. Consequences of Fluid Extraction on the Silicate Mantle and Structure of Europa

Removal of Fe ± S from the devolatilized deep interior at the Fe-FeS eutectic (Section 2.3), and calculation of Europa's structure with PlanetProfile using the resulting core and residual silicate mantle thermodynamic properties (Section 2.4) yields a spherical shell structure, MoI (0.3455–0.3457) and density consistent with present-day Europa observations, assuming a ~ 30 km ice shell (Figure 1; Text S4). Further details about the predicted deep mineralogy are found in Text S5 and Figures S12 and S13. Figure S16 shows the density, heat capacity, and bulk and shear moduli of resulting profiles.

## 4. Concluding Remarks

We find that the resulting volatile mass evolved from Europa's deep interior is consistent with, and can even exceed, the hydrosphere's present mass. The size and composition of the ocean depend on the assumed accreted composition of Europa. Different bulk compositions lead to different mineralogies in the thermodynamic model, that mediate the escape of volatiles and solutes. To elaborate:

1. Building a volatile mass equivalent to that of Europa's current hydrosphere by prograde metamorphism prior to core formation was probable if Europa accreted a disproportionately large amount of CI or CM chondrite material, water, and/or cometary material relative to the expected abundance of these materials at Jupiter's location in the early Solar System (cf., Desch et al., 2018). Other known chondritic materials have insufficient volatile mass extractable by metamorphism to account for Europa's present hydrosphere mass (Section 2.1 & Section 3.1).
2. Europa's ocean, if derived from thermal evolution of the interior as shown here, was carbon and sulfur-rich (Section 3.1). If thermal excursions in the interior (from radioactive decay and tidal dissipation) were unimportant since differentiation, geochemical equilibrium models predict that the ocean would remain CO<sub>2</sub>, carbonate and CaSO<sub>4</sub>-rich (Section 3.2). However, pressure has a first order effect on the ocean's composition: decreasing pressure precipitates gypsum, removing calcium and sulfur from solution, thereby increasing the relative concentration of chlorine further up the water column, such that Cl > S at  $\lesssim 10$  MPa. Thickening of the ice shell preferentially freezes in SO<sub>4</sub><sup>2-</sup>, rejecting and concentrating Cl at the base of the ice shell in time (Marion et al., 2005), leaving the relative concentration of SO<sub>4</sub><sup>2-</sup> unchanged at depth.
3. While the volatile mass in the initially accreted bulk body was high (Section 3.1), the deep interior must be relatively volatile-poor at present to meet the MoI and density constraints (Section 3.3). Therefore, prograde metamorphism and fluid migration into the hydrosphere was necessarily efficient in order to remove volatile mass from the interior. Volatile loss from the rocky interior in excess of the present hydrosphere mass can be accommodated by early loss to space, especially because of the high pCO<sub>2</sub> outgassed. Alternatively, a large portion of volatiles (particularly CO<sub>2</sub>) would be retained in clathrates, and their periodic destabilization by tidal heating may provide oxidants and buoyant pressure at the ice-ocean interface. We rule out complete ocean freeze-out enabled by the thermal blanketing effect of a stable seafloor clathrate layer: even if a thick clathrate layer is stable at the seafloor over geologic time,  $\lesssim 80$  km thick high pressure ice layers at Ganymede and Titan with heat fluxes > 6 mW/m<sup>2</sup> from the silicate interior are able to maintain a liquid ocean (Kalousová & Sotin, 2020). Melt and heat transport from the bottom of the clathrate layer to the ocean would occur either through hot plume conduits or solid state convection (Choblet et al., 2017; Kalousová & Sotin, 2020).
4. The CO<sub>2</sub>-rich ocean delivered by metamorphism may facilitate life's emergence by contributing to the generation of a proton gradient between acidic ocean water and alkaline hydrothermal fluids (Camprubi et al., 2019), if the latter are present in Europa.

While these updated models are enabled by modern computational thermodynamics and data, we expect that further work will refine these results prior to the arrival of the JUICE and Europa Clipper missions in the coming decade. In particular, 4.5 Gyr of tidally mediated magmatism may have continued to modify the

deep interior, possibly driving solid-state mantle convection, volcanism, and volatile element redistribution and loss (Běhounková et al., 2021). The oxidized ocean may have been reduced in time with hydrogen generated by serpentinization enabled by thermal cracking (Vance et al., 2016), but better constraints on the conditions of fracture formation and propagation are required (Klimczak et al., 2019). Further improvements to the thermodynamic data of high pressure H<sub>2</sub>O-CO<sub>2</sub> phases (Abramson et al., 2018) and their integration with thermodynamic models (e.g., Perple\_X) are also needed to assess the build-up of the ocean: the stability of such phases can be the factor dictating whether an ocean world will be habitable (Marounina & Rogers, 2020). Finally, we have also made the simplifying assumption that fluid percolation from depth was efficient. A coupled tidal-thermodynamic-geodynamic model would more accurately determine fluid retained-to-extracted ratios.

## Data Availability Statement

All data are available through Zenodo: <https://doi.org/10.5281/zenodo.5218908>. AccretR is available through Melwani Daswani (2020). PlanetProfile is available through <https://zenodo.org/record/4052711>. Rcrust is available through Mayne et al. (2016) and <https://tinyurl.com/rcrust>.

## Acknowledgments

M. Melwani Daswani thanks Jinping Hu, Paul Byrne, Orenthal Tucker, Evan Carnahan and the Origins and Habitability Laboratory (JPL) for discussions, Saikiran Tharimena for codes, Hauke Hussmann for tidal dissipation data, and James Connolly for help with the Perple\_X code. The authors thank JPL research interns Marika Leitner and Garret Levine for early contributions to this work. This work was supported by NASA through the Europa Clipper Project to S. D. Vance and C. R. Glein, and NASA grant NN-H18ZDA001N-HW:Habitable Worlds awarded to M. Melwani Daswani and S. D. Vance. M. Melwani Daswani and S. Vance were also supported by the NASA Astrobiology Institute's Icy Worlds initiative (13-13NAI7\_2-0024). A part of this research was carried out at the Jet Propulsion Laboratory, California Institute of Technology, under a contract with the National Aeronautics and Space Administration (80NM0018D0004). Copyright 2021. All rights reserved.

## References

- Abramson, E. H., Bollengier, O., Brown, J. M., Journaux, B., Kaminsky, W., & Pakhomova, A. (2018). Carbonic acid monohydrate. *American Mineralogist*, 103(9), 1468–1472. <https://doi.org/10.2138/am-2018-655410.2138/am-2018-6554>
- Anderson, J. D., Schubert, G., Jacobson, R. A., Lau, E. L., Moore, W. B., & Sjogren, W. L. (1998). Europa's differentiated internal structure: Inferences from four Galileo encounters. *Science*, 281(5385), 2019–2022. <https://doi.org/10.1126/science.281.5385.2019>
- Barr, A. C., & Canup, R. M. (2008). Constraints on gas giant satellite formation from the interior states of partially differentiated satellites. *Icarus*, 198(1), 163–177. <https://doi.org/10.1016/j.icarus.2008.07.004>
- Běhounková, M., Tobie, G., Choblet, G., Kervazo, M., Melwani Daswani, M., Dumoulin, C., & Vance, S. D. (2021). Tidally induced magmatic pulses on the oceanic floor of Jupiter's moon Europa. *Geophysical Research Letters*, 48, e2020GL090077. <https://doi.org/10.1029/2020GL090077>
- Bierson, C. J., & Nimmo, F. (2020). Explaining the Galilean satellites' density gradient by hydrodynamic escape. *The Astrophysical Journal*, 897, L43. <https://doi.org/10.3847/2041-8213/aba11a>
- Bland, M. T., Showman, A. P., & Tobie, G. (2008). The production of Ganymede's magnetic field. *Icarus*, 198(2), 384–399. <https://doi.org/10.1016/j.icarus.2008.07.011>
- Brown, M. E., & Hand, K. P. (2013). Salts and radiation products on the surface of Europa. *The Astronomical Journal*, 145(4), 110. <https://doi.org/10.1088/0004-6256/145/4/110>
- Camprubi, E., de Leeuw, J. W., House, C. H., Raulin, F., Russell, M. J., Spang, A., et al. (2019). The emergence of life. *Space Science Reviews*, 215(8), 56. <https://doi.org/10.1007/s11214-019-0624-8>
- Canup, R. M., & Ward, W. R. (2002). Formation of the Galilean satellites: Conditions of accretion. *The Astronomical Journal*, 124(6), 3404–3423. <https://doi.org/10.1086/344684>
- Canup, R. M., & Ward, W. R. (2009). Origin of Europa and the Galilean satellites. In R. T. Pappalardo, W. B. McKinnon, & K. Khurana (Eds.), *Europa* (pp. 59–83). Tucson, AZ: University of Arizona Press.
- Choblet, G., Tobie, G., Sotin, C., Kalousová, K., & Grasset, O. (2017). Heat transport in the high-pressure ice mantle of large icy moons. *Icarus*, 285, 252–262. <https://doi.org/10.1016/j.icarus.2016.12.002>
- Connolly, J. A. D. (2005). Computation of phase equilibria by linear programming: A tool for geodynamic modeling and its application to subduction zone decarbonation. *Earth and Planetary Science Letters*, 236(1–2), 524–541. <https://doi.org/10.1016/j.epsl.2005.04.033>
- Connolly, J. A. D. (2009). The geodynamic equation of state: What and how. *Geochemistry, Geophysics, Geosystems*, 10(10). <https://doi.org/10.1029/2009gc002540>
- Connolly, J. A. D., & Galvez, M. E. (2018). Electrolytic fluid speciation by Gibbs energy minimization and implications for subduction zone mass transfer. *Earth and Planetary Science Letters*, 501, 90–102. <https://doi.org/10.1016/j.epsl.2018.08.024>
- Dalton, J. B., Cassidy, T., Paranicas, C., Shirley, J. H., Prockter, L. M., & Kamp, L. W. (2013). Exogenic controls on sulfuric acid hydrate production at the surface of Europa. In *Surfaces, Atmospheres and Magnetospheres of the Outer Planets and Their Satellites and Ring Systems: Part VIII, Planetary and Space Science*, 77, 45–63. <https://doi.org/10.1016/j.pss.2012.05.013>
- Desch, S. J., Kalyaan, A., & Alexander, C. M. O. (2018). The effect of Jupiter's formation on the distribution of refractory elements and inclusions in Meteorites. *The Astrophysical Journal Supplement Series*, 238(1), 11. <https://doi.org/10.3847/1538-4365/aad95f>
- Erkaev, N., Lammer, H., Elkins-Tanton, L., Stökl, A., Odert, P., Marq, E., et al. (2014). Escape of the martian protoatmosphere and initial water inventory. *Planetary evolution and life*, 98, 106–119. <https://doi.org/10.1016/j.pss.2013.09.008>
- Estrada, P. R., Mosqueira, I., Lissauer, J. J., D'Angelo, G., & Cruikshank, D. (2009). Formation of Jupiter and conditions for accretion of the Galilean satellites. In R. T. Pappalardo, W. B. McKinnon, & K. Khurana (Eds.), *Europa* (pp. 27–58). Tucson, AZ: University of Arizona Press.
- Fischer, P. D., Brown, M. E., Trumbo, S. K., & Hand, K. P. (2016). Spatially resolved spectroscopy of Europa's large-scale compositional units at 3–4 m with Keck NIRSPEC. *The Astronomical Journal*, 153(1), 13. <https://doi.org/10.3847/1538-3881/153/1/13>
- Gaidos, E. J., Nealon, K. H., & Kirschvink, J. L. (1999). Life in ice-covered oceans. *Science*, 284(5420), 1631–1633. <https://doi.org/10.1126/science.284.5420.1631>
- Galvez, M. E., Manning, C. E., Connolly, J. A., & Rumble, D. (2015). The solubility of rocks in metamorphic fluids: A model for rock-dominated conditions to upper mantle pressure and temperature. *Earth and Planetary Science Letters*, 430, 486–498. <https://doi.org/10.1016/j.epsl.2015.06.019>

- Glein, C. R., Postberg, F., & Vance, S. D. (2018). The geochemistry of Enceladus: Composition and controls. In *Enceladus and the icy moons of Saturn*. The University of Arizona Press. [https://doi.org/10.2458/azu\\_uapress\\_9780816537075-ch003](https://doi.org/10.2458/azu_uapress_9780816537075-ch003)
- Gorce, J., Caddick, M., & Bodnar, R. (2019). Thermodynamic constraints on carbonate stability and carbon volatility during subduction. *Earth and Planetary Science Letters*, 519, 213–222. <https://doi.org/10.1016/j.epsl.2019.04.047>
- Greeley, R., Chyba, C. F., Head, J., McCord, T., McKinnon, W. B., & Pappalardo, R. T. (2004). Geology of Europa. In *Jupiter: The planet, satellites and magnetosphere* (pp. 329–362). New York: Cambridge University Press.
- Hand, K., Carlson, R., & Chyba, C. (2007). Energy, chemical disequilibrium, and geological constraints on Europa. *Astrobiology*, 7(6), 1006–1022. <https://doi.org/10.1089/ast.2007.0156>
- Hansen, G. B., & McCord, T. B. (2008). Widespread CO<sub>2</sub> and other non-ice compounds on the anti-Jovian and trailing sides of Europa from Galileo/NIMS observations. *Geophysical Research Letters*, 35, L01202. <https://doi.org/10.1029/2007GL031748>
- Huss, G. R., Rubin, A. E., & Grossman, J. N. (2006). Thermal metamorphism in chondrites. In D. S. Lauretta, & H. Y. McSween (Eds.), *Meteorites and the early solar system II* (pp. 567–586). Tucson, AZ: University of Arizona Press. <https://doi.org/10.2307/j.ctv1vzdzmm.34>
- Hussmann, H., & Spohn, T. (2004). Thermal-orbital evolution of Io and Europa. *Icarus*, 171(2), 391–410. <https://doi.org/10.1016/j.icarus.2004.05.020>
- Kalousová, K., & Sotin, C. (2020). Dynamics of Titan's high-pressure ice layer. *Earth and Planetary Science Letters*, 545, 116416. <https://doi.org/10.1016/j.epsl.2020.116416>
- Kargel, J. S. (1991). Brine volcanism and the interior structures of asteroids and icy satellites. *Icarus*, 94(2), 368–390. [https://doi.org/10.1016/0019-1035\(91\)90235-1](https://doi.org/10.1016/0019-1035(91)90235-1)
- Kargel, J. S., Kaye, J. Z., Head, J. W., Marion, G. M., Sassen, R., Crowley, J. K., et al. (2000). Europa's crust and ocean: Origin, composition, and the prospects for life. *Icarus*, 148(1), 226–265. <https://doi.org/10.1006/icar.2000.6471>
- Klimczak, C., Byrne, P. K., Regensburger, P. V., Bohnenstiehl, D. R., Hauck, S. A. II, Dombard, A. J., & Elder, C. M. (2019). Strong ocean floors within Europa, Titan, and Ganymede limit geological activity there; Enceladus less so. Retrieved from <https://ui.adsabs.harvard.edu/abs/2019LP....50.2912K>
- Kuramoto, K., & Matsui, T. (1994). Formation of a hot proto-atmosphere on the accreting giant icy satellite: Implications for the origin and evolution of Titan, Ganymede, and Callisto. *Journal of Geophysical Research*, 99, 21183–21200. <https://doi.org/10.1029/94JE01864>
- Kuskov, O., & Kronrod, V. (2005). Internal structure of Europa and Callisto. *Icarus*, 177(2), 550–569. <https://doi.org/10.1016/j.icarus.2005.04.014>
- Leitner, M. A., & Lunine, J. I. (2019). Modeling early Titan's ocean composition. *Icarus*, 333, 61–70. <https://doi.org/10.1016/j.icarus.2019.05.008>
- Ligier, N., Poulet, F., Carter, J., Brunetto, R., & Gougeot, F. (2016). VLT/SINFONI observations of Europa: New insights into the surface composition. *The Astronomical Journal*, 151(6), 163. <https://doi.org/10.3847/0004-6256/151/6/163>
- Lobo, A. H., Thompson, A. F., Vance, S. D., & Tharimena, S. (2021). A pole-to-equator ocean overturning circulation on Enceladus. *Nature Geoscience*, 14(4), 185–189. <https://doi.org/10.1038/s41561-021-00706-3>
- Lunine, J. I., & Nolan, M. C. (1992). A massive early atmosphere on Triton. *Icarus*, 100, 221–234. [https://doi.org/10.1016/0019-1035\(92\)90031-2](https://doi.org/10.1016/0019-1035(92)90031-2)
- Lunine, J. I., & Stevenson, D. J. (1982). Formation of the galilean satellites in a gaseous nebula. *Icarus*, 52(1), 14–39. [https://doi.org/10.1016/0019-1035\(82\)90166-x](https://doi.org/10.1016/0019-1035(82)90166-x)
- Makalkin, A. B., Dorofeeva, V. A., & Ruskol, E. L. (1999). Modeling the protosatellite Circum-Jovian accretion disk: An estimate of the basic parameters. *Solar System Research*, 33, 456.
- Manthilake, G., Bolfan-Casanova, N., Novella, D., Mookherjee, M., & Andraut, D. (2016). Dehydration of chlorite explains anomalously high electrical conductivity in the mantle wedges. *Science Advances*, 2, e1501631. <https://doi.org/10.1126/sciadv.1501631>
- Marion, G. M., Kargel, J. S., Catling, D. C., & Jakubowski, S. D. (2005). Effects of pressure on aqueous chemical equilibria at subzero temperatures with applications to Europa. *Geochimica et Cosmochimica Acta*, 69(2), 259–274. <https://doi.org/10.1016/j.gca.2004.06.024>
- Marounina, N., & Rogers, L. A. (2020). Internal structure and CO<sub>2</sub> reservoirs of habitable water worlds. *The Astrophysical Journal*, 890, 107. <https://doi.org/10.3847/1538-4357/ab68e4>
- Mayne, M. J., Moyer, J.-F., Stevens, G., & Kaislaniemi, L. (2016). Rcrust: A tool for calculating path-dependent open system processes and application to melt loss. *Journal of Metamorphic Geology*, 34(7), 663–682. <https://doi.org/10.1111/jmg.12199>
- McCord, T. B., Hansen, G. B., Fanale, F. P., Carlson, R. W., Matson, D. L., Johnson, T. V., et al. (1998). Salts on Europa's surface detected by Galileo's near infrared mapping spectrometer. *Science*, 280, 1242, 1245. <https://doi.org/10.1126/science.280.5367.1242>
- McKinnon, W. B., & Zolensky, M. E. (2003). Sulfate content of Europa's ocean and shell: Evolutionary considerations and some geological and astrobiological implications. *Astrobiology*, 3, 879–897. <https://doi.org/10.1089/153110703322736150>
- Miller, K. E., Glein, C. R., & Waite, J. H. (2019). Contributions from accreted organics to Titan's atmosphere: New insights from cometary and chondritic data. *The Astrophysical Journal*, 871(1), 59. <https://doi.org/10.3847/1538-4357/aaf561>
- Moore, W. B., & Hussmann, H. (2009). Thermal evolution of Europa's silicate interior. In R. T. Pappalardo, W. B. McKinnon & K. Khurana (Eds.), *Europa*. (pp. 369–380). Tucson: University of Arizona Press.
- Mosqueira, I., Estrada, P., & Turrini, D. (2010). Planetesimals and satellitesimals: Formation of the satellite systems. *Space Science Reviews*, 153, 431–446. <https://doi.org/10.1007/s11214-009-9614-6>
- Néri, A., Guyot, F., Reynard, B., & Sotin, C. (2020). A carbonaceous chondrite and cometary origin for icy moons of Jupiter and Saturn. *Earth and Planetary Science Letters*, 530, 115920. <https://doi.org/10.1016/j.epsl.2019.115920>
- Odert, P., Lammer, H., Erkaev, N., Nikolaou, A., Lichtenegger, H., Johnstone, C., et al. (2018). Escape and fractionation of volatiles and noble gases from Mars-sized planetary embryos and growing protoplanets. *Icarus*, 307, 327–346. <https://doi.org/10.1016/j.icarus.2017.10.031>
- Pan, D., Spanu, L., Harrison, B., Sverjensky, D. A., & Galli, G. (2013). Dielectric properties of water under extreme conditions and transport of carbonates in the deep Earth. *Proceedings of the National Academy of Sciences*, 110, 6646–6650. <https://doi.org/10.1073/pnas.1221581110>
- Pasek, M. A., & Greenberg, R. (2012). Acidification of Europa's subsurface ocean as a consequence of oxidant delivery. *Astrobiology*, 12(2), 151–159. <https://doi.org/10.1089/ast.2011.0666>
- Reed, M. H. (1998). Calculation of simultaneous chemical equilibria in aqueous-mineral-gas systems and its application to modeling hydrothermal processes. In J. P. Richards (Ed.), *Techniques in hydrothermal ore deposits geology* (Vol. 10, pp. 109–124). Littleton, CO: Society of Economic Geologists, Inc. <https://doi.org/10.5382/rev.10.05>
- Richard, G., Monnerieu, M., & Rabinowicz, M. (2007). Slab dehydration and fluid migration at the base of the upper mantle: Implications for deep earthquake mechanisms. *Geophysical Journal International*, 168(3), 1291–1304. <https://doi.org/10.1111/j.1365-246X.2006.03244.x>
- Ronnet, T., & Johansen, A. (2020). Formation of moon systems around giant planets: Capture and ablation of planetesimals as foundation for a pebble accretion scenario. *Astronomy & Astrophysics*, 633, A93. <https://doi.org/10.1051/0004-6361/201936804>

- Ronnet, T., Mousis, O., & Vernazza, P. (2017). Pebble accretion at the origin of water in Europa. *The Astrophysical Journal*, *845*, 92. <https://doi.org/10.3847/1538-4357/aa80e6>
- Roth, L., Saur, J., Retherford, K. D., Strobel, D. F., Feldman, P. D., McGrath, M. A., & Nimmo, F. (2014). Transient water vapor at Europa's south pole. *Science*, *343*(6167), 171. <https://doi.org/10.1126/science.1247051>
- Schubert, G., Sohl, F., & Hussmann, H. (2009). Interior of Europa. In R. T. Pappalardo, W. B. McKinnon & K. Khurana (Eds.), *Europa* (pp. 353–367). Tucson: University of Arizona Press.
- Sohl, F., Spohn, T., Breuer, D., & Nagel, K. (2002). Implications from galileo observations on the interior structure and chemistry of the galilean satellites. *Icarus*, *157*(1), 104–119. <https://doi.org/10.1006/icar.2002.6828>
- Sparks, W. B., Hand, K. P., McGrath, M. A., Bergeron, E., Cracraft, M., & Deustua, S. E. (2016). Probing for evidence of plumes on Europa with HST/STIS. *The Astrophysical Journal*, *829*, 121. <https://doi.org/10.3847/0004-637X/829/2/121>
- Tan, S., Sekine, Y., Shibuya, T., Miyamoto, C., & Takahashi, Y. (2021). The role of hydrothermal sulfate reduction in the sulfur cycles within Europa: Laboratory experiments on sulfate reduction at 100MPa. *Icarus*, *357*, 114222. <https://doi.org/10.1016/j.icarus.2020.114222>
- Tobie, G., Choblet, G., & Sotin, C. (2003). Tidally heated convection: Constraints on Europa's ice shell thickness. *Journal of Geophysical Research*, *108*(E11), 5124. <https://doi.org/10.1029/2003JE002099>
- Tobie, G., Mocquet, A., & Sotin, C. (2005). Tidal dissipation within large icy satellites: Applications to Europa and Titan. *Europa Icy Shell*, *177*(2), 534–549. <https://doi.org/10.1016/j.icarus.2005.04.006>
- Townsend, M., & Huber, C. (2020). A critical magma chamber size for volcanic eruptions. *Geology*, *48*(5), 431–435. <https://doi.org/10.1130/G47045.1>
- Trumbo, S. K., Brown, M. E., Fischer, P. D., & Hand, K. P. (2017). A new spectral feature on the trailing hemisphere of Europa at 3.78  $\mu$ m. *The Astronomical Journal*, *153*(6), 250. <https://doi.org/10.3847/1538-3881/aa6d80>
- Trumbo, S. K., Brown, M. E., & Hand, K. P. (2019). Sodium chloride on the surface of Europa. *Science Advances*, *5*(6), eaaw7123. <https://doi.org/10.1126/sciadv.aaw7123>
- Vance, S. D., Hand, K. P., & Pappalardo, R. T. (2016). Geophysical controls of chemical disequilibria in Europa. *Geophysical Research Letters*, *43*(10), 4871–4879. <https://doi.org/10.1002/2016GL068547>
- Vance, S. D., Panning, M. P., Stähler, S., Cammarano, F., Bills, B. G., Tobie, G., et al. (2018). Geophysical investigations of habitability in ice-covered ocean worlds. *Journal of Geophysical Research: Planets*, *123*(1), 180–205. <https://doi.org/10.1002/2017je005341>
- Wakita, S., & Genda, H. (2019). Fates of hydrous materials during planetesimal collisions. *Icarus*, *328*, 58–68. <https://doi.org/10.1016/j.icarus.2019.03.008>
- Zahnle, K. J., & Catling, D. C. (2017). The cosmic shoreline: The evidence that escape determines which planets have atmospheres, and what this may mean for proxima centauri B. *The Astrophysical Journal*, *843*, 122. <https://doi.org/10.3847/1538-4357/aa7846>
- Zolotov, M. Y., & Kargel, J. S. (2009). On the chemical composition of Europa's icy shell, ocean, and underlying rocks. In R. T. Pappalardo, W. B. McKinnon, & K. Khurana (Eds.), *Europa* (pp. 431). Tucson: University of Arizona Press. Retrieved from <https://uapress.arizona.edu/book/europa>
- Zolotov, M. Y., & Shock, E. L. (2001). Composition and stability of salts on the surface of Europa and their oceanic origin. *Journal of Geophysical Research*, *106*(E12), 32815–32827. <https://doi.org/10.1029/2000JE001413>
- Zolotov, M. Y., & Shock, E. L. (2004). A model for low-temperature biogeochemistry of sulfur, carbon, and iron on Europa. *Journal of Geophysical Research*, *109*(E6), E06003. <https://doi.org/10.1029/2003JE002194>

## References From the Supporting Information

- Airieu, S., Farquhar, J., Thiemens, M., Leshin, L., Bao, H., & Young, E. (2005). Planetary sulfide and aqueous alteration in CM and CI carbonaceous chondrites. *Geochimica et Cosmochimica Acta*, *69*(16), 4167–4172. <https://doi.org/10.1016/j.gca.2005.01.029>
- Badro, J., Brodholt, J. P., Piet, H., Siebert, J., & Ryerson, F. J. (2015). Core formation and core composition from coupled geochemical and geophysical constraints. *Proceedings of the National Academy of Sciences of the United States of America*, *112*(40), 12310–12314. <https://doi.org/10.1073/pnas.1505672112>
- Bardyn, A., Baklouti, D., Cottin, H., Fray, N., Briois, C., Paquette, J., & Hilchenbach, M. (2017). Carbon-rich dust in comet 67P/Churyumov-Gerasimenko measured by COSIMA/Rosetta. *Monthly Notices of the Royal Astronomical Society*, *469*, S712–S722. <https://doi.org/10.1093/mnras/stx2640>
- Bjerga, A. (2014). *Evolution of talc- and carbonate-bearing alterations in ultramafic rocks on Leka (central Norway)* (Doctoral dissertation). Bergen: The University of Bergen. Retrieved from <https://hdl.handle.net/1956/7893>
- Bjerga, A., Konopásek, J., & Pedersen, R. (2015). Talc-carbonate alteration of ultramafic rocks within the Leka Ophiolite complex, Central Norway. *Lithos*, *227*, 21–36. <https://doi.org/10.1016/j.lithos.2015.03.016>
- Bland, P. A., Cressy, G., & Menzies, O. N. (2004). Modal mineralogy of carbonaceous chondrites by X-ray diffraction and Mössbauer spectroscopy. *Meteoritics & Planetary Science*, *39*, 3–16. <https://doi.org/10.1111/j.1945-5100.2004.tb00046.x>
- Bouquet, A., Mousis, O., Glein, C. R., Danger, G., & Waite, J. H. (2019). The role of clathrate formation in Europa's ocean composition. *The Astrophysical Journal*, *885*(1), 14. <https://doi.org/10.3847/1538-4357/ab40b0>
- Brearely, A. J. (2006). The action of water. *Meteorites and the early solar system II* (pp. 584). Retrieved from <https://ui.adsabs.harvard.edu/abs/2006mess.book.584B>
- Bretscher, A., Hermann, J., & Pettke, T. (2018). The influence of oceanic oxidation on serpentinite dehydration during subduction. *Earth and Planetary Science Letters*, *499*, 173–184. <https://doi.org/10.1016/j.epsl.2018.07.017>
- Cerpa, N. G., Padrón-Navarta, J. A., & Arcay, D. (2020). *Uncertainties in the stability field of UHP hydrous phases (10-A phase and phase E) and deep-slab dehydration: Potential implications for fluid migration and water fluxes at subduction zones.* <https://doi.org/10.5194/egusphere-egu2020-4783>
- Chatterjee, N. D., & Froese, E. (1975). A thermodynamic study of the pseudobinary join muscovite-paragonite in the system KAlSi<sub>3</sub>O<sub>8</sub>-NaAlSi<sub>3</sub>O<sub>8</sub>-Al<sub>2</sub>O<sub>3</sub>-SiO<sub>2</sub>-H<sub>2</sub>O. *American Mineralogist*, *60*(11–12), 985–993.
- Clay, P. L., Burgess, R., Busemann, H., Ruzié-Hamilton, L., Joachim, B., Day, J. M. D., & Ballentine, C. J. (2017). Halogens in chondritic meteorites and terrestrial accretion. *Nature*, *551*(7682), 614–618. <https://doi.org/10.1038/nature24625>
- Connolly, J. A. D., & Podladchikov, Y. Y. (1998). Compaction-driven fluid flow in viscoelastic rock. *Geodinamica Acta*, *11*, 55–84. <https://doi.org/10.1080/09853111.1998.11105311>
- Craddock, R. A., & Greeley, R. (2009). Minimum estimates of the amount and timing of gases released into the martian atmosphere from volcanic eruptions. *Icarus*, *204*(2), 512–526. <https://doi.org/10.1016/j.icarus.2009.07.026>

- Day, J. M., Corder, C. A., Assayag, N., & Cartigny, P. (2019). Ferrous oxide-rich asteroid achondrites. *Geochimica et Cosmochimica Acta*. <https://doi.org/10.1016/j.gca.2019.04.005>
- Dhooghe, F., De Keyser, J., Altwegg, K., Briois, C., Balsiger, H., Berthelier, J.-J., et al. (2017). Halogens as tracers of protosolar nebula material in comet 67P/Churyumov–Gerasimenko. *Monthly Notices of the Royal Astronomical Society*, *472*(2), 1336–1345. <https://doi.org/10.1093/mnras/stx1911>
- Ferrand, T. P., Hilaret, N., Incel, S., Deldicque, D., Labrousse, L., Gasc, J., et al. (2017). Dehydration-driven stress transfer triggers intermediate-depth earthquakes. *Nature Communications*, *8*(1), 15247. <https://doi.org/10.1038/ncomms15247>
- Flynn, G. J., Consolmagno, G. J., Brown, P., & Macke, R. J. (2018). Physical properties of the stone meteorites: Implications for the properties of their parent bodies. *Geochemistry*, *78*(3), 269–298. <https://doi.org/10.1016/j.chemer.2017.04.002>
- Fowler, A. P., Zierenberg, R. A., Reed, M. H., Palandri, J., Óskarsson, F., & Gunnarsson, I. (2019a). Rare earth element systematics in boiled fluids from basalt-hosted geothermal systems. *Geochimica et Cosmochimica Acta*, *244*, 129–154. <https://doi.org/10.1016/j.gca.2018.10.001>
- Fredriksson, K., & Kerridge, J. F. (1988). Carbonates and sulfates in CI chondrites — Formation by aqueous activity on the parent body. *Meteoritics*, *23*, 35–44. <https://doi.org/10.1111/j.1945-5100.1988.tb00894.x>
- Freedman, A. J. E., Bird, D. K., Arnorsson, S., Fridriksson, T., Elders, W. A., & Fridleifsson, G. O. (2009). Hydrothermal minerals record CO<sub>2</sub> partial pressures in the Reykjanes geothermal system, Iceland. *American Journal of Science*, *309*(9), 788–833. <https://doi.org/10.2475/09.2009.02>
- Frost, B. R. (1991). Chapter 1. Introduction to oxygen fugacity and its petrological importance. In D. H. Lindsley (Ed.), *Oxide minerals* (pp. 1–10). Berlin, Boston: De Gruyter. <https://doi.org/10.1515/9781501508684-004>
- García-Arias, M. (2020). Consistency of the activity–composition models of Holland, Green, and Powell (2018) with experiments on natural and synthetic compositions: A comparative study. *Journal of Metamorphic Geology*, *38*, 993–1010. <https://doi.org/10.1111/jmg.12557>
- Gounelle, M., & Zolensky, M. E. (2001). A terrestrial origin for sulfate veins in CI1 chondrites. *Meteoritics & Planetary Science*, *36*, pp. 1321–1329. <https://doi.org/10.1111/j.1945-5100.2001.tb01827.x>
- Green, E., Holland, T. J. B., & Powell, R. (2007). An order-disorder model for omphacitic pyroxenes in the system jadeite-diopside-hedenbergite-acmite, with applications to eclogitic rocks. *American Mineralogist*, *92*(7), 1181–1189. <https://doi.org/10.2138/am.2007.2401>
- Holland, T. J. B., Baker, J., & Powell, R. (1998). Mixing properties and activity–composition relationships of chlorites in the system MgO–FeO–Al<sub>2</sub>O<sub>3</sub>–SiO<sub>2</sub>–H<sub>2</sub>O. *European Journal of Mineralogy*, *10*(3), 395–406. <https://doi.org/10.1127/ejm/10/3/0395>
- Holland, T. J. B., Green, E. C. R., & Powell, R. (2018). Melting of peridotites through to Granites: A simple thermodynamic model in the system KNCFMASHTOCr. *Journal of Petrology*, *59*(5), 881–900. <https://doi.org/10.1093/petrology/egy048>
- Jennings, E. S., Holland, T. J. B., Shorttle, O., Maclennan, J., & Gibson, S. A. (2016). The Composition of melts from a heterogeneous mantle and the origin of Ferropicrite: Application of a thermodynamic model. *Journal of Petrology*. <https://doi.org/10.1093/petrology/egw065>
- Jia, X., Kivelson, M. G., Khurana, K. K., & Kurth, W. S. (2018). Evidence of a plume on Europa from Galileo magnetic and plasma wave signatures. *Nature Astronomy*, *2*(6), 459–464. <https://doi.org/10.1038/s41550-018-0450-z>
- Lammer, H., Chassefière, E., Karatekin, O., Morschhauser, A., Niles, P. B., Mousis, O., et al. (2013). Outgassing history and escape of the Martian atmosphere and Water Inventory. *Space Science Reviews*, *174*(1–4), 113–154. <https://doi.org/10.1007/s11214-012-9943-8>
- Lammer, H., Selsis, F., Chassefière, E., Breuer, D., Griefmeier, J.-M., Kulikov, Y. N., et al. (2010). Geophysical and atmospheric evolution of habitable planets. *Astrobiology*, *10*, 45–68. <https://doi.org/10.1089/ast.2009.0368>
- Leclère, H., Faulkner, D., Llana-Fúnez, S., Bedford, J., & Wheeler, J. (2018). Reaction fronts, permeability and fluid pressure development during dehydration reactions. *Earth and Planetary Science Letters*, *496*, 227–237. <https://doi.org/10.1016/j.epsl.2018.05.005>
- Le Roy, L., Altwegg, K., Balsiger, H., Berthelier, J.-J., Bieler, A., Briois, C., et al. (2015). Inventory of the volatiles on comet 67P/Churyumov–Gerasimenko from Rosetta/ROSINA. *Astronomy & Astrophysics*, *583*, A1. <https://doi.org/10.1051/0004-6361/201526450>
- Li, J., & Fei, Y. (2014). 3.15 — Experimental constraints on core composition. In H. D. Holland & K. K. Turekian (Eds.), *Treatise on geochemistry* (2nd ed., pp. 527–557). Oxford: Elsevier. <https://doi.org/10.1016/b978-0-08-095975-7.00214-x>
- Lodders, K., & Fegley, B. (1998). *The planetary scientist's companion*. New York: Oxford University Press.
- McCord, T. B., Hansen, G. B., Matson, D. L., Johnson, T. V., Crowley, J. K., Fanale, F. P., et al. (1999). Hydrated salt minerals on Europa's surface from the Galileo near-infrared mapping spectrometer (NIMS) investigation. *Journal of Geophysical Research*, *104*, 11827–11851. <https://doi.org/10.1029/1999JE900005>
- Melwani Daswani, M. (2020). *AccretR*. Zenodo. <https://doi.org/10.5281/ZENODO.3827540>
- Menzel, M. D., Garrido, C. J., & López Sánchez-Vizcaino, V. (2020). Fluid-mediated carbon release from serpentinite-hosted carbonates during dehydration of antigorite-serpentinite in subduction zones. *Earth and Planetary Science Letters*, *531*, 115964. <https://doi.org/10.1016/j.epsl.2019.115964>
- Miller, S., van der Zee, W., Olgaard, D., & Connolly, J. (2003). A fluid-pressure feedback model of dehydration reactions: Experiments, modeling, and application to subduction zones. In *Physical properties of rocks and other geomaterials, a special volume to honour professor H. Kern* (Vol. 370, pp. 241–251). [https://doi.org/10.1016/s0040-1951\(03\)00189-6](https://doi.org/10.1016/s0040-1951(03)00189-6)
- Nozaka, T., Wintsch, R. P., & Meyer, R. (2017). Serpentinization of olivine in troctolites and olivine gabbros from the Hess deep rift. *Lithos*, *282–283*, 201–214. <https://doi.org/10.1016/j.lithos.2016.12.032>
- Padrón-Navarta, J. A., Sánchez-Vizcaino, V. L., Hermann, J., Connolly, J. A., Garrido, C. J., Gómez-Pugnaire, M. T., & Marchesi, C. (2013). Tschermak's substitution in antigorite and consequences for phase relations and water liberation in high-grade serpentinites. *Lithos*, *178*, 186–196. <https://doi.org/10.1016/j.lithos.2013.02.001>
- Palandri, J. L., & Reed, M. H. (2004). Geochemical models of metasomatism in ultramafic systems: Serpentinization, rodingitization, and sea floor carbonate chimney precipitation. *Geochimica et Cosmochimica Acta*, *68*(5), 1115–1133. <https://doi.org/10.1016/j.gca.2003.08.006>
- Palme, H., Lodders, K., & Jones, A. (2014). 2.2 — Solar system abundances of the elements. In H. D. Holland & K. K. Turekian (Eds.), *Treatise on geochemistry* (2nd ed., pp. 15–36). Oxford: Elsevier. <https://doi.org/10.1016/b978-0-08-095975-7.00118-2>
- Pätzold, M., Andert, T., Hahn, M., Asmar, S. W., Barriot, J.-P., Bird, M. K., et al. (2016). A homogeneous nucleus for comet 67P/Churyumov–Gerasimenko from its gravity field. *Nature*, *530*(7588), 63–65. <https://doi.org/10.1038/nature16535>
- Pitzer, K. S., & Sterner, S. M. (1994). Equations of state valid continuously from zero to extreme pressures for H<sub>2</sub>O and CO<sub>2</sub>. *The Journal of Chemical Physics*, *101*(4), 3111–3116. <https://doi.org/10.1063/1.467624>
- Prieto-Ballesteros, O., Kargel, J. S., Fernández-Sampedro, M., Selsis, F., Martínez, E. S., & Hogenboom, D. L. (2005). Evaluation of the possible presence of clathrate hydrates in Europa's icy shell or seafloor. *Europa Icy Shell*, *177*(2), 491–505. <https://doi.org/10.1016/j.icarus.2005.02.021>

- Saxena, S., & Eriksson, G. (2015). Thermodynamics of Fe-S at ultra-high pressure. *Calphad*, 51, 202–205. <https://doi.org/10.1016/j.calphad.2015.09.009>
- Scott, H., Williams, Q., & Ryerson, F. (2002). Experimental constraints on the chemical evolution of large icy satellites. *Earth and Planetary Science Letters*, 203(1), 399–412. [https://doi.org/10.1016/S0012-821X\(02\)00850-6](https://doi.org/10.1016/S0012-821X(02)00850-6)
- Singerling, S. A., & Brearley, A. J. (2018). Primary iron sulfides in CM and CR carbonaceous chondrites: Insights into nebular processes. *Meteoritics & Planetary Science*, 53, 2078–2106. <https://doi.org/10.1111/maps.13108>
- Sloan, E. D., & Koh, C. A. (2008). Clathrate hydrates of natural gases (3rd ed., 752). Boca Raton, FL: CRC Press.
- Sonzogni, Y., Treiman, A. H., & Schwenzer, S. P. (2017). Serpentinite with and without brucite: A reaction pathway analysis of a natural serpentinite in the Josephine ophiolite, California. *Journal of Mineralogical and Petrological Sciences*, 112(2), 59–76. <https://doi.org/10.2465/jmps.160509>
- Sotin, C., Grasset, O., & Mocquet, A. (2007). Mass-radius curve for extrasolar Earth-like planets and ocean planets. *Icarus*, 191(1), 337–351. <https://doi.org/10.1016/j.icarus.2007.04.006>
- Sotin, C., & Tobie, G. (2004). Internal structure and dynamics of the large icy satellites. *Comptes Rendus Physique*, 5(7), 769–780. <https://doi.org/10.1016/j.crhy.2004.08.001>
- Steenstra, E. S., & van Westrenen, W. (2018). A synthesis of geochemical constraints on the inventory of light elements in the core of Mars. *Icarus*, 315, 69–78. <https://doi.org/10.1016/j.icarus.2018.06.023>
- Sverjensky, D. A., Harrison, B., & Azzolini, D. (2014). Water in the deep Earth: The dielectric constant and the solubilities of quartz and corundum to 60 kb and 1200°C. *Geochimica et Cosmochimica Acta*, 129, 125–145. <https://doi.org/10.1016/j.gca.2013.12.019>
- Tian, F., Kasting, J. F., & Solomon, S. C. (2009). Thermal escape of carbon from the early Martian atmosphere. *Geophysical Research Letters*, 36, L02205. <https://doi.org/10.1029/2008GL036513>
- Verba, C., O'Connor, W., Rush, G., Palandri, J., Reed, M., & Ideker, J. (2014). Geochemical alteration of simulated wellbores of CO<sub>2</sub> injection sites within the Illinois and Pasco Basins. *International Journal of Greenhouse Gas Control*, 23, 119–134. <https://doi.org/10.1016/j.ijggc.2014.01.015>
- Walder, P., & Pelton, A. D. (2005). Thermodynamic modeling of the Fe-S system. *Journal of Phase Equilibria and Diffusion*, 26(1), 23–38. <https://doi.org/10.1007/s11669-005-0055-y>
- Warner, M. (2004). Free water and seismic reflectivity in the lower continental crust. *Journal of Geophysics and Engineering*, 1(1), 88–101. <https://doi.org/10.1088/1742-2132/1/1/012>
- Wilson, C. R., Spiegelman, M., van Keken, P. E., & Hacker, B. R. (2014). Fluid flow in subduction zones: The role of solid rheology and compaction pressure. *Earth and Planetary Science Letters*, 401, 261–274. <https://doi.org/10.1016/j.epsl.2014.05.052>
- Wood, B. J., Li, J., & Shahar, A. (2013). Carbon in the core: Its influence on the properties of core and mantle. *Reviews in Mineralogy and Geochemistry*, 75(1), 231–250. <https://doi.org/10.2138/rmg.2013.75.8>
- Zhang, H. (2003). Internal structure models and dynamical parameters of the Galilean satellites. *Celestial Mechanics and Dynamical Astronomy*, 87(1), 189–195. <https://doi.org/10.1023/A:1026188029324>
- Zolensky, M., Barrett, R., & Browning, L. (1993). Mineralogy and composition of matrix and chondrule rims in carbonaceous chondrites. *Geochimica et Cosmochimica Acta*, 57(13), 3123–3148. [https://doi.org/10.1016/0016-7037\(93\)90298-b](https://doi.org/10.1016/0016-7037(93)90298-b)